OPEN ACCESS
IOP Publishing | International Atomic Energy Agency
Nuclear Fusion
Nucl. Fusion **57** (2017) 116041 (9pp)
https://doi.org/10.1088/1741-4326/aa796e

Plasma–wall interaction studies within the EUROfusion consortium: progress on plasma-facing components development and qualification

S. Brezinsek[1], J.W. Coenen[1], T. Schwarz-Selinger[2], K. Schmid[2], A. Kirschner[1], A. Hakola[3], F.L. Tabares[4], H.J. van der Meiden[5], M.-L. Mayoral[6], M. Reinhart[1], E. Tsitrone[7], T. Ahlgren[31], M. Aints[20], M. Airila[3], S. Almaviva[30], E. Alves[24], T. Angot[9], V. Anita[15], R. Arredondo Parra[2], F. Aumayr[18], M. Balden[2], J. Bauer[2], M. Ben Yaala[12], B.M. Berger[18], R. Bisson[9], C. Björkas[31], I. Bogdanovic Radovic[28], D. Borodin[1], J. Bucalossi[7], J. Butikova[23], B. Butoi[27], I. Čadež[25], R. Caniello[17], L. Caneve[30], G. Cartry[9], N. Catarino[24], M. Čekada[25], G. Ciraolo[7], L. Ciupinski[13], F. Colao[30], Y. Corre[7], C. Costin[15], T. Craciunescu[27], A. Cremona[17], M. De Angeli[17], A. de Castro[4], R. Dejarnac[22], D. Dellasega[11], P. Dinca[27], T. Dittmar[1], C. Dobrea[27], P. Hansen[1], A. Drenik[2,25], T. Eich[2], S. Elgeti[2], D. Falie[27], N. Fedorczak[7], Y. Ferro[9], T. Fornal[21], E. Fortuna-Zalesna[13], L. Gao[2], P. Gasior[21], M. Gherendi[27], F. Ghezzi[17], Ž. Gosar[33], H. Greuner[2], E. Grigore[27], C. Grisolia[7], M. Groth[8], M. Gruca[21], J. Grzonka[13], J.P. Gunn[7], K. Hassouni[26], K. Heinola[31], T. Höschen[2], S. Huber[19], W. Jacob[2], I. Jepu[27], X. Jiang[1], I. Jogi[20], A. Kaiser[19], J. Karhunen[8], M. Kelemen[25], M. Köppen[1], H.R. Koslowski[1], A. Kreter[1], M. Kubkowska[21], M. Laan[20], L. Laguardia[17], A. Lahtinen[31], A. Lasa[31], V. Lazic[30], N. Lemahieu[32], J. Likonen[3], J. Linke[32], A. Litnovsky[1], Ch. Linsmeier[1], T. Loewenhoff[32], C. Lungu[27], M. Lungu[27], G. Maddaluno[30], H. Maier[2], T. Makkonen[8], A. Manhard[2], Y. Marandet[7], S. Markelj[25], L. Marot[12], C. Martin[9], A.B. Martin-Rojo[4], Y. Martynova[1], R. Mateus[24], D. Matveev[1], M. Mayer[2], G. Meisl[2], N. Mellet[7], A. Michau[26], J. Miettunen[8], S. Möller[1], T.W. Morgan[5], J. Mougenot[26], M. Mozetič[25], V. Nemanič[25], R. Neu[2], K. Nordlund[31], M. Oberkofler[2], E. Oyarzabal[4], M. Panjan[25], C. Pardanaud[9], P. Paris[20], M. Passoni[11], B. Pegourie[7], P. Pelicon[25], P. Petersson[16], K. Piip[20], G. Pintsuk[32], G.O. Pompilian[27], G. Popa[15], C. Porosnicu[27], G. Primc[25], M. Probst[19], J. Räisänen[31], M. Rasinski[1], S. Ratynskaia[16], D. Reiser[1], D. Ricci[17], M. Richou[7], J. Riesch[2], G. Riva[33], M. Rosinski[21], P. Roubin[9], M. Rubel[16], C. Ruset[27], E. Safi[31], G. Sergienko[1], Z. Siketic[28], A. Sima[27], B. Spilker[32], R. Stadlmayr[18], I. Steudel[32], P. Ström[16], T. Tadic[28], D. Tafalla[4], I. Tale[23], D. Terentyev[29], A. Terra[1], V. Tiron[15], I. Tiseanu[27], P. Tolias[16], D. Tskhakaya[18], A. Uccello[17], B. Unterberg[1], I. Uytdenhoven[29], E. Vassallo[17], P. Vavpetič[25], P. Veis[14], I.L. Velicu[15], J.W.M. Vernimmen[5], A. Voitkans[23], U. von Toussaint[2], A. Weckmann[16], M. Wirtz[32], A. Založnik[25], R. Zaplotnik[25] and WP PFC contributors[a]

[a] see www.euro-fusionscipub.org/PFC

[1] Forschungszentrum Jülich GmbH, Institut für Energie und Klimaforschung—Plasmaphysik, Partner of the Trilateral Euregio Cluster (TEC), 52425 Jülich, Germany
[2] Max-Planck-Institut für Plasmaphysik, D-85748 Garching, Germany
[3] VTT Technical Research Centre of Finland Ltd., PO Box 1000, FI-02044 VTT, Finland
[4] Association EURATOM-CIEMAT, Av. Complutense 22, 28040 Madrid, Spain
[5] DIFFER Dutch Institute for Fundamental Energy Research, De Zaale 20, 5612 AJ Eindhoven, Netherlands
[6] CCFE Fusion Association, Culham Science Centre, Abingdon, OX143DB, United Kingdom
[7] CEA, IRFM, F-13108 Saint Paul Lez Durance, France
[8] Department of Applied Physics, Aalto University, PO Box 14100, FI-00076 Aalto, Finland
[9] Aix-Marseille Univ. CNRS, PIIM, F13013 Marseille, France
[10] Department of Applied Physics UG (Ghent University), St-Pietersnieuwstraat 4,1 B-9000 Ghent, Belgium
[11] Dipartimento di Energia, Politecnico di Milano, Milan, Italy
[12] Swiss Plasma Center (SPC), Ecole Polytechnique Fédérale de Lausanne (EPFL), CH-1015 Lausanne, Switzerland
[13] Faculty of Materials Science and Engineering, Warsaw University of Technology, Woloska 141, 02-507 Warsaw, Poland
[14] Faculty of Mathematics, Physics and Informatics, Department of Experimental Physics, Comenius University, Mlynska dolina F2, 84248 Bratislava, Slovakia
[15] Faculty of Physics, 'Al. I. Cuza' University, 700506 Iasi, Romania
[16] Fusion Plasma Physics, EES, KTH Royal Institute of Technology, SE-10044 Stockholm, Sweden
[17] Institute of Plasma Physics 'P.Caldirola', National Research Council of Italy, via R. Cozzi 53, 20125 Milan, Italy
[18] Institut für Angewandte Physik, Technische Universität Wien, Wiedner Hauptstraße 8-10, 1040 Wien, Österreich
[19] Institut für Ionen- und Angewandte Physik, Universität Innsbruck, Technikerstraße 25, 6020 Innsbruck, Österreich
[20] Institute of Physics, University of Tartu, W. Ostwaldi street 1, Tartu 50411, Estonia
[21] Institute of Plasma Physics and Laser Microfusion, Hery 23, 01-497 Warsaw, Poland
[22] Institute of Plasma Physics of the CAS, Za Slovankou 1782/3, 182 00 Praha 8, Czechia
[23] Institute of Solid State Physics (University of Latvia), Kengaraga 8, LV-1063, Riga, Latvia
[24] Instituto de Plasmas e Fusaó Nuclear, Instituto Superior Técnico, Universidade de Lisboa, Portugal
[25] Jožef Stefan Institute, Jamova Cesta 39, SI-1000 Ljubljana, Slovenia
[26] Laboratoire des Sciences des Procédés et des Matériaux (LSPM); CNRS, Université Paris 13, Sorbonne Paris Cité, F-93430 Villetaneuse, France
[27] National Institute for Laser, Plasma and Radiation Physics, 409 Atomistilor Street, Magurele, 077125, Romania
[28] Rudjer Boškovic Institute, Bijenicka cesta 54, HR-10000 Zagreb, Croatia
[29] SCK · CEN, Nuclear Materials Science Institute, Boeretang 200, Mol, 2400, Belgium
[30] Department of Fusion and Technology for Nuclear Safety and Security- ENEA C. R. Frascati - via E. Fermi 45, 00044 Frascati (Roma), Italy
[31] Department of Physics, University of Helsinki, PO Box 64, FI-00014 University of Helsinki, Finland
[32] Forschungszentrum Jülich GmbH, Institut für Energie und Klimaforschung—IEK-2, 52425 Jülich, Germany
[33] Jožef Stefan International Postgraduate School, Jamova 39, 1000 Ljubljana, Slovenia

E-mail: s.brezinsek@fz-juelich.de

Received 15 December 2016, revised 17 May 2017
Accepted for publication 14 June 2017
Published 18 August 2017

Abstract

The provision of a particle and power exhaust solution which is compatible with first-wall components and edge-plasma conditions is a key area of present-day fusion research and mandatory for a successful operation of ITER and DEMO. The work package plasma-facing components (WP PFC) within the European fusion programme complements with laboratory experiments, i.e. in linear plasma devices, electron and ion beam loading facilities, the studies performed in toroidally confined magnetic devices, such as JET, ASDEX Upgrade, WEST etc. The connection of both groups is done via common physics and engineering studies, including the qualification and specification of plasma-facing components, and by modelling codes that simulate edge-plasma conditions and the plasma–material interaction as well as the study of fundamental processes. WP PFC addresses these critical points in order to ensure reliable and efficient use of conventional, solid PFCs in ITER (Be and W) and DEMO (W and steel)

with respect to heat-load capabilities (transient and steady-state heat and particle loads), lifetime estimates (erosion, material mixing and surface morphology), and safety aspects (fuel retention, fuel removal, material migration and dust formation) particularly for quasi-steady-state conditions. Alternative scenarios and concepts (liquid Sn or Li as PFCs) for DEMO are developed and tested in the event that the conventional solution turns out to not be functional. Here, we present an overview of the activities with an emphasis on a few key results: (i) the observed synergistic effects in particle and heat loading of ITER-grade W with the available set of exposition devices on material properties such as roughness, ductility and microstructure; (ii) the progress in understanding of fuel retention, diffusion and outgassing in different W-based materials, including the impact of damage and impurities like N; and (iii), the preferential sputtering of Fe in EUROFER steel providing an *in situ* W surface and a potential first-wall solution for DEMO.

Keywords: plasma-facing components, plasma-surface interaction, power exhaust, particle exhaust, tungsten, beryllium

(Some figures may appear in colour only in the online journal)

1. Introduction

Particle and power exhaust is a key area of current fusion research and mandatory for the successful operation of ITER and DEMO—the first reactor-like device. The importance of this area, as well as the need to provide a solution for the plasma-facing interface, has been identified in Europe in the so-called fusion roadmap [1] resulting in a dedicated programme covering tokamaks as well as laboratory research studies in linear plasma devices, electron-beam, neutral-beam, and ion-beam loading facilities. The interconnection of both research areas is done via common experimental physics studies, specification and qualification of plasma-facing components (PFCs) in different loading facilities, and most importantly, by simulation of plasma exhaust and plasma–material interaction [2] starting from basic process modeling, e.g. molecular dynamics (MD [3]), to integrated tokamak modelling, e.g. global erosion-deposition codes like ERO [4] (modelling volume covers tens of cm range in poloidal, toridal and radial directions) or WallDYN [5] (modelling volume covers the full tokamak) and plasma boundary codes (SOLPS [2], SOLEDGE-EIRENE [6] etc). Thereby, the plasma and particle exhaust solution must ensure the compatibility of the PFC power handling with plasma-edge conditions required for good plasma confinement during quasi steady-state operation for hundreds of plasma seconds as foreseen in ITER and beyond [7]. Laboratory heat-load facilities (JUDITH [8], GLADIS [9] etc) and linear plasmas (PSI-2 [10], Pilot-PSI [11], MAGNUM etc) are presently essential to predict PFC performance at high particle fluence $\phi > 10^{27} \mathrm{D}^{+}\mathrm{m}^{-2}$) and the number of thermal cycles ($>10^{6}$ ELM-like events) as expected in such quasi-state conditions. Current experiments in JET [12] and ASDEX Upgrade [13] are used to verify solutions for tens of plasma seconds without active cooling of PFCs, but long-pulse steady-state operations in the complex tokamak environment will be available in the near future in WEST [14] for studies complementary to the corresponding laboratory experiments.

The EUROfusion work package ‘preparation of efficient PFC operation for ITER and DEMO’ or in short ‘PFC’, the successor of the EFDA task force for plasma–wall interaction (TF PWI) [15], addresses these critical points in order to ensure the reliable and efficient use of conventional (solid metallic) plasma-facing components in ITER (made of tungsten and beryllium [16]) and DEMO (made of tungsten and reduced-activation ferritic martensitic (RAFM) steel [17]) with respect to heat load capabilities (transient and steady-state heat and particle loads), lifetime estimates (erosion, material mixing, and surface morphology) and safety aspects (fuel retention, fuel removal, material migration, and dust formation). Thereby, the development of plasma-edge and plasma–surface interaction diagnostics used to determine physics quantities, such as electron density, electron temperature, ion energy or impinging ion flux and composition is performed in a dedicated supporting activity providing crucial input in particular to modelling activities. Successfully qualified diagnostics or concepts such as laser-induced breakdown spectroscopy (LIBS), optimised to determine the fuel content (mixed hydrogenic fuel and helium) and material composition in metallic plasma-facing materials exposed to divertor-like plasma conditions [18], will be transferred to the tokamak environment. These different activities are coordinated within six sub projects all aiming to support the conventional PFC solution with solid metallic components and i.e. a full tungsten divertor following the step ladder approach (AUG to JET to ITER to DEMO). In addition, one sub project is following the back-up solution via liquid metals [19] as alternative PFC concept to deal with the high power loads at high wall temperatures in DEMO, to ensure the required low fuel retention to close the fuel cycle in the reactor. The current qualification is focused in Europe on the capillary porous system (CPS), which shows promising results in small scale components whereas tests with large scale divertor components have not yet been executed. Also, the impact of liquid metals on the plasma performance have not yet been tested. We present in the following sections a few key results of the coordinated

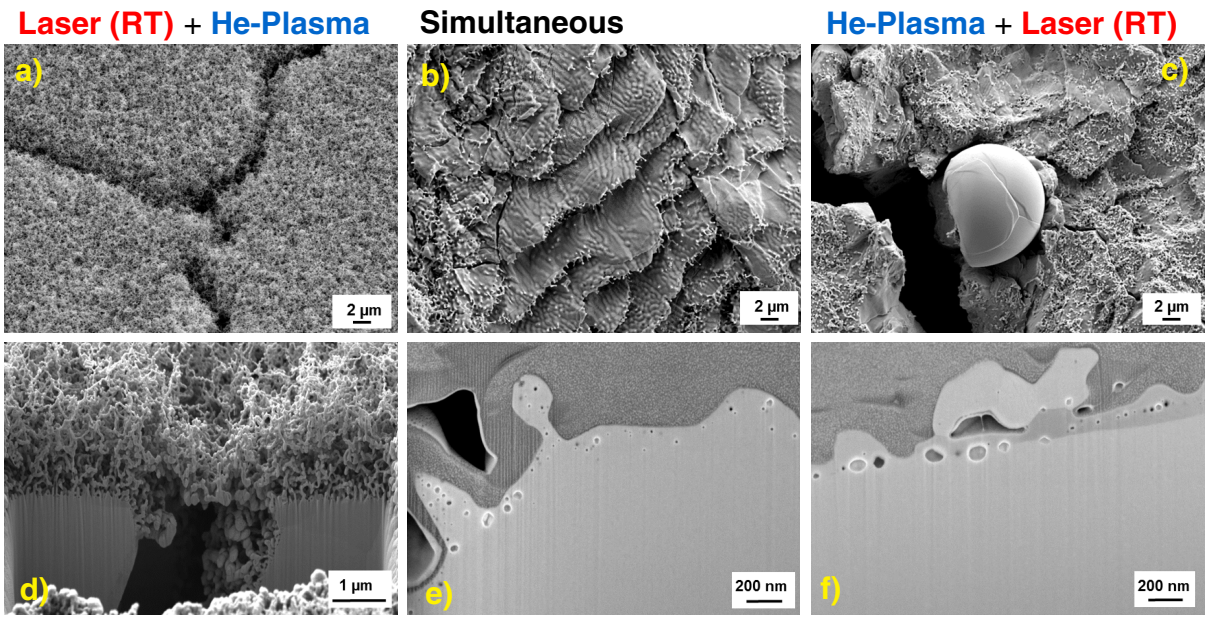

Figure 1. Scanning electron microscope images and focused ion beam cuts of He-plasma and laser-exposed surfaces: (*a*) and (*d*) First laser at room temperature, then He plasma exposure at 1120 K; (*b*) and (*e*) simultaneous laser and He-plasma exposure at 1120 K; (*c*) and (*f*) First He plasma at 1120 K then laser exposure at room temperature [20]. Reproduced from [20]. CC BY-NC-ND 4.0.

studies within WP PFC that addresses ITER and DEMO related issues.

2. Synergistic effects in heat and particle loading of W

One of the most critical questions of transient heat load experiments on ITER-relevant materials like tungsten, is whether the obtained limits can be extended to power and heat flux conditions expected during ELM excursions in the divertor. Most available techniques can match single parameters (e.g. the heat flux factor), but full experimental matching of the power and particle flux densities, the impact energy spectrum, the plasma conditions and impurity composition expected in ITER cannot be achieved. A series of experiments with combined particle and heat load on reference W plasma-facing material were carried out to identify synergistic effects with respect to material properties such as hardness, ductility, and microstructure as well as erosion, retention and mixing by load execution in sequence or simultaneously. In combination with loading parameters such as the surface temperature with a detailed mapping of the impact of accompanying synergy effects, e.g. with helium or hydrogen exposure, could be documented [20], leading to a complex modification of material properties featuring reduced cracking behaviour in the combined plasma and heat flux exposure by laser beam in comparison with conventional thermal shock tests in electron beam facilities. Figure 1 provides the change of W surface morphology by applying (i) first, 1000 laser pulses with a power density of 0.76 GWm^{-2} at a maximum temperature of $T = 1120$ K followed by PSI-2 plasma exposure in helium (He ion impact energy: $E_{in} = 80$ eV, flux: $\Gamma = 2.8 \times He^{+}10^{22}$ $m^{-2}s^{-1}$, and fluence: $\phi = 5.6 \times 10^{25}$ He^{+} m^{-2}); (ii) simultaneous exposure under similar heat pulse and plasma conditions; and (iii) reversed order with initial plasma exposure followed by ELM-like heat pulses by laser exposition. The order of exposure determines the final state of surface modification with W nanostructure formation on the cracked W sample in condition (i), a complex surface structure with remains of the W nanostructure and He nanobubbles in (ii), and surface roughness, near-surface melting and He nanobubbles in (iii). Further details of the experiment and its analysis are described in [20]. Corresponding experiments in H plasmas as well as the comparison of heat pulses by e-beam, neutral beam, laser and high energy plasma bursts simulating all ELM-like conditions is provided in [21].

These experimental results are leading to a better physics understanding of the impact mechanisms during PFC exposure and are used to develop model descriptions. The latter are then used for predictions of PFC capabilities and operational space, but exposure under tokamak conditions are still desirable to verify the obtained models for ITER and DEMO. Indeed WEST experiments with the associated installations of diagnostics are prepared to bridge laboratory and tokamak experiments and to increase the predictability of PFC performance with minimization of operational risks for ITER.

3. Material migration and W prompt re-deposition

The understanding of material migration, thus the process cycle of material erosion, transport, and deposition is one of the key issues for a successful and safe operation of ITER. The process cycle is associated with the lifetime of first wall material components, predominantly by erosion, and with the safety aspect due to long-term tritium retention and dust formation and release [22]. The latter is in JET as well as in ITER dominated by co-deposition of tritium with Be [23] whereas implantation in W will determine the retention in a

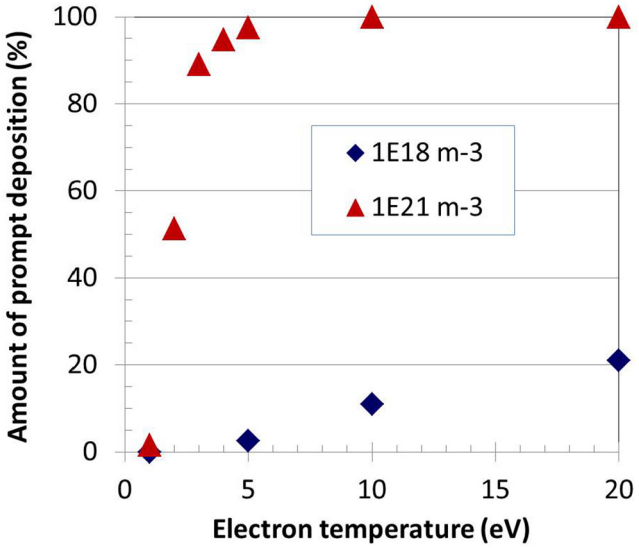

Figure 2. Modelled amounts of prompt deposition in dependence on the electron temperature for two different electron densities (1×10^{18} m^{-3} and 1×10^{21} m^{-3}) [24]. Reproduced with permission from [24].

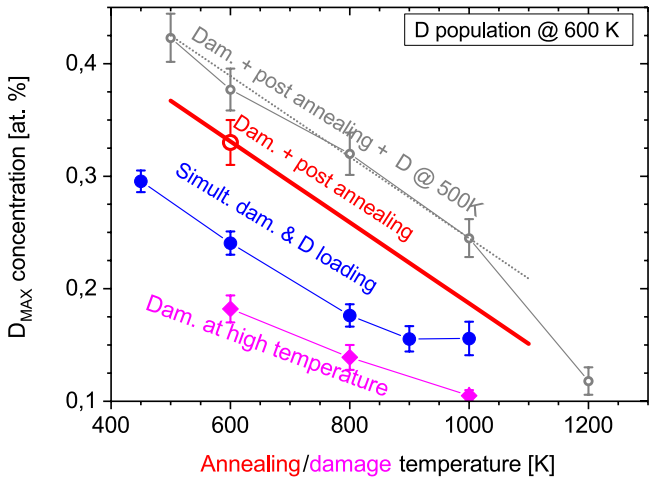

Figure 3. Maximum D concentration obtained at the position of the maximum of the peak displacement damage profile versus damage temperatures obtained from D depth profiles for the damaging at high temperatures (process (i)) and simultaneous self-damaging and D loading. The data are compared to damaging at room temperature and afterward post-damaging annealing and defect population by D: damaging process (ii) (grey data) and extrapolation for population of defects at 600 K (red data). Reproduced from [43]. CC BY-NC-ND 4.0.

full metallic DEMO. The description of the cycle and initial predictions to the material migration and retention pattern in ITER assuming H-mode plasmas in D was successfully done by the WallDYN [5] and ERO [4] codes within WP PFC.

Concerning the life time estimation of W PFCs, emphasis in the ERO modelling was put on description of prompt re-deposition of W, thus the return of eroded and ionized W within one Larmour radius [24]. The inclusion of an improved sheath description obtained from PIC calculations [25] in ERO was used to perform parameter studies covering the typical operational space of the JET tokamak in order to provide the prompt re-deposition fraction of W. ERO modelling of the prompt deposition of sputtered tungsten atoms has been done for an electron temperature (T_e) range of 1 eV to 20 eV and electron density (n_e) range from 1×10^{18} m^{-3} to 1×10^{21} m^{-3}. A magnetic field of 3 T with a shallow field angle of 2° relative to the surface has been used. The resulting fractions of prompt deposition are summarised in figure 2. For typical JET inter-ELM plasmas ($T_e = 10$ eV, 1×10^{19} to 1×10^{20} m^{-3} the fraction of prompt deposition is between 60% and 90%, which is in fair agreement with experimental observations. During ELM conditions with n_e of 1×10^{20} and T_e of 20 eV the modelled amount of prompt deposition is about 95%. For this simulation the 'free-streaming model' [26] has been applied, assuming a deuterium ion energy of 1 keV. The self-sputtering yield of returning tungsten ions has been calculated and it seems that for the parameter range studied, the yield will always be well below one therefore runaway sputtering does not occur.

The next step in global migration predictions will expand from pure D plasmas in a pure Be/W environment towards a plasma with realistic impurity mixture and include the new laboratory findings on synergistic effects of Ne, N (seeding gas) and He (ash), on erosion, fuel retention and material mixing such as Be_3N_2 [27] or WN production [28], identified to act as a diffusion barrier and formation of co-deposits with Be/D/N.

Moreover, dedicated studies on ammonia formation to better understand its production in the plasma and the metallic first wall [29–32], to assess its potential risk and develop possible mitigation procedures, in case nitrogen needs to be used as seeding gas for divertor cooling in the future are also covered. Fundamental studies related to outgassing and the isotope exchange in W, Be and mixed Be–W co-deposits are performed in conjunction with a PISCES-B collaboration [33]. Mixed Be layers have been developed [34] to mimic JET co-deposits and allow the successful qualification of *in situ* fuel retention diagnostics such as LIBS and fuel-removal techniques such as baking. Reference analysis of the fuel content in plasma-facing materials with post-mortem techniques such as thermal desorption spectroscopy (TDS) and nuclear reaction analysis (NRA) [35] are used to provide standard values for experiments and modelling as well as to benchmark the quantification with laser-based diagnostics such as LIBS [36–38] and laser-induced desorption spectroscopy (LIDS) [39].

4. Fuel retention studies in self-damaged W

Until recently, all hydrogen retention studies were performed by sequential high energy ion damaging and subsequent plasma/gas/atom loading of the material by hydrogen isotopes. Detailed studies were performed in WP PFC to experimentally determine the retention mechanisms, the isotope exchange, the surface release mechanisms as well as to develop corresponding complex models for these processes in bare plasma-facing materials and co-deposits [40, 41]. However, in a real fusion-reactor environment, implantation of energetic hydrogen ions and neutrals as well as damage creation by neutron irradiation will take place at the same time. The consequences of synergistic effects for hydrogen retention in tungsten are unknown, but theory predicts a defective stabilization in the presence of hydrogen atoms

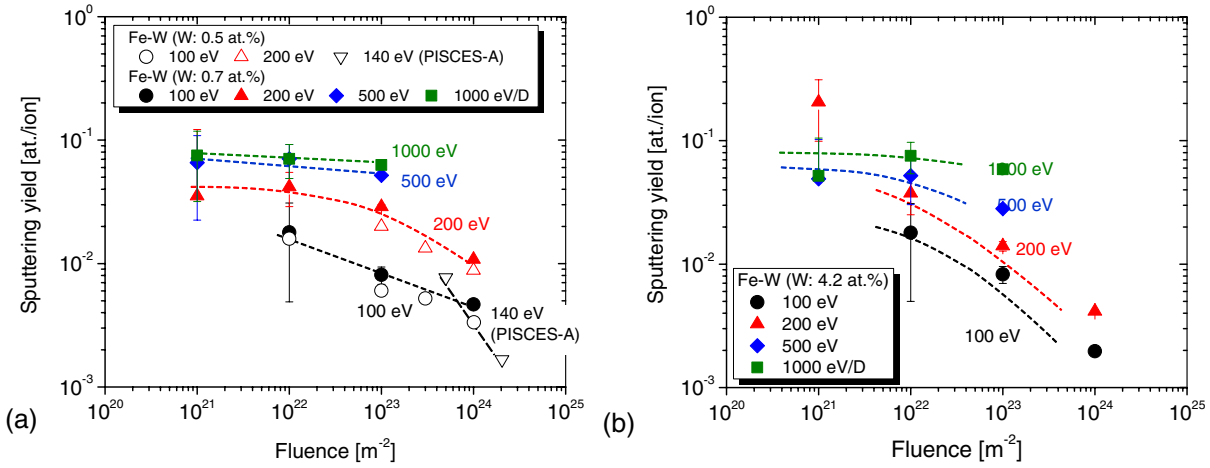

Figure 4. Fluence dependence of sputtering yields of Fe–W layers with (*a*) low W concentrations (0.5 and 0.7 at.%) and (*b*) high W concentration (W concentration: 4.2 at.%) [44]. Reprinted from [44], Copyright 2015, with permission from Elsevier.

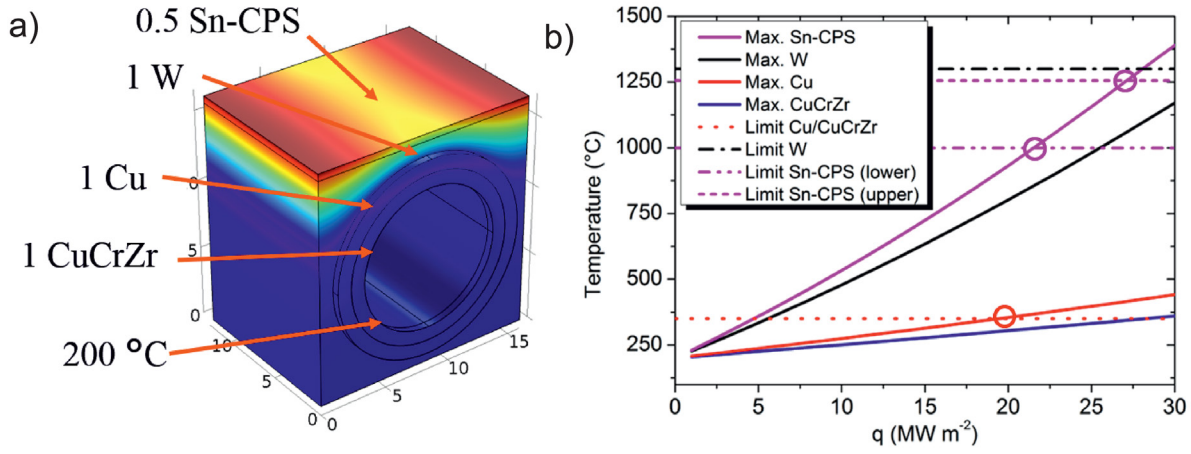

Figure 5. (*a*) COMSOL model of a Sn CPS and W based mono block design for DEMO. The inner wall temperature of the water pipe is also shown. (*b*) The maximum equilibrium temperature for each part of the component and their material temperature limits. The intersection of the limits is shown with a circle [50, 51]. Reproduced from [50]. CC BY-NC-ND 4.0.

in tungsten [42]. To take one step further towards a more realistic situation, we have performed the first experimental study on simultaneous defect creation by 10.8 MeV W self-ion implantation and D-atom-beam loading ($E = 0.28$ eV, $\Gamma = 5.4 \times 10^{18}\mathrm{Dm}^{-2}\mathrm{s}^{-1}$) in W between 450 K and 1000 K. After the damaging and loading, D depth profiles were measured by NRA using the $\mathrm{D}(^3\mathrm{He}, p)^4\mathrm{He}$ reaction. In order to determine how many traps were actually created in the material, the samples were simultaneously damaged and loaded and the NRA analysis was exposed to D atoms for an additional 19 h at 600 K, $\phi = 3.7 \times 10^{23}\mathrm{Dm}^{-2}$. As expected, the highest concentration was obtained for the 450 K case, decreasing with damaging temperature. In order to sort out the observed effects, a comparison to a series of sequential damaging/annealing/exposure experiments was made [43], as depicted in figure 3. Namely, three sequential experimental series were performed in addition with different damaging/exposure procedures, that help to separate the processes: (i) W-ion damaging at elevated temperatures + D-atom exposure at 600 K afterwards to determine the trap concentration; (ii) W-ion damaging at room temperature + sample post-damaging annealing at different temperatures for one hour + D-atom loading at 500 K afterwards to determine the trap concentration; and (iii) W-ion damaging at room temperature + D-atom exposure at elevated temperatures afterwards. Comparison of the maximum deuterium concentration obtained at the maximum of the peak displacement damage for simultaneous self-damaging and D-atom loading and processes under (i) and (ii) are shown in figure 3. Synergistic effects were observed, namely, higher D concentrations were found in the case of simultaneous damaging and D-atom loading as compared to sequential damaging at elevated temperatures and populating the defects afterwards. However, the deuterium retention is still lower compared to sequential damaging at room temperature and post-damaging annealing. The observations are explained by stabilization of the created defects by the presence of solute hydrogen in the simultaneous case, in the bulk that would annihilate at high temperatures without the presence of hydrogen.

5. Preferential sputtering of Fe–W and EUROFER

An example for pure DEMO research within WP PFC are erosion studies on RAFM steels, such as EUROFER, which are foreseen as a primary structural material. In certain areas of the main chamber wall in DEMO, such as on blanket modules tungsten was foreseen as thin protection coating on the structural steel to minimize wall erosion which would otherwise be too high due to Fe in the steel potentially leading to high-Z accumulation in the plasma. Recently, EUROFER was proposed directly as plasma-facing material in recessed areas as it provides lower fuel retention and less weight, which would simplify the design and hence reduce cost as well as reduce the risk of coating failures. The reason for RAFM to be applicable is that amongst other elements, it contains small amounts of W (0.33 at.%) whose sputtering behaviour will be smaller compared to those of the lighter elements. W is therefore expected to enrich at the surface during the course of operation which would lead to a reduction of the sputter yield with exposition time. To understand the effect quantitatively a model system of W containing Fe layers was developed and exposed in addition to EUROFER to different D ion beams and plasmas to study the erosion in the impact energy range between 100 eV and 1 keV, target temperatures between room temperature and 770 K for D fluxes between $10^{17}D^{+}\ m^{-2}s^{-1}$ and $10^{21}D^{+}m^{-2}s^{-1}$ collecting up to a fluence of $6 \times 10^{25}D^{+}m^{-2}$. To measure erosion and W surface enrichment mass loss, Rutherford backscattering spectrometry (RBS), time-of-flight heavy ion elastic recoil detection analysis (ToF HIERDA), as well as secondary ion mass spectrometry (SIMS) were applied. All experiments confirmed the anticipated effect and have proven the W enrichment at the surface at room temperature. Enrichment is at maximum when the impact energy is below the sputter threshold for physical sputtering of W (200 eV for D^{+}, 140 eV for T^{+}) but is observed also above. At room temperature and for an energy of 200 eV D^{-1} at fluences of $10^{22}D^{+}m^{-2}$ enrichment is already observed and saturates at $3 \times 10^{24}D^{+}m^{-2}$. Figure 4(*a*) shows the sputter yields as function of D fluence for different energies of the Fe–W model-system films with different initial W concentrations [44]. However, a quantitative comparison between modelling and experiment is hampered by the limited depth resolution. Presently medium energy and low energy ion scattering (MEIS and LEIS) is applied to improve this [45]. A recently developed code that combines the simulation of the ion–solid interaction with solid state diffusion predicts that diffusion will set in above 800 K [46] and will counteract enrichment [47]. However, it is doubtful if it is justified to apply the tracer diffusion coefficient for tungsten in Fe for a multi component material such as RAFM steel. Therefore, reliable experiments at higher temperatures need to be conducted in the future and in addition, a task was started to measure the diffusion coefficient as a function of W concentration. First experiments show that 800 K might indeed be the critical operation temperature for RAFM steels as PFM material which is just at the nominal wall temperature of DEMO.

6. Liquid metals as alternative PFCs for DEMO

Qualification studies with respect to power loads, erosion rates and fuel retention/removal rates of liquid plasma-facing material solutions made of Sn, Li or Sn/Li alloys were carried out in close relation with design studies dedicated to a new European divertor test tokamak, an intermediate step to DEMO, equipped with a non-conventional divertor [19]. Dedicated plasma compatibility studies with CPS made of LiSn alloys were performed in TJ-II in order to study the fuel retention, hydrogen recycling, and plasma compatibility. Indeed low fuel retention of below $0.01\% = \frac{H}{Sn+Li}$ at $T < 720$ K was measured by TDS. No substantial impact on the plasma operation was observed with intact CPS, whereas plasma operation was hampered if the stainless steel structure with liquid metal was exposed [48, 49]. Another important question for liquid metals is, if the power handling capability can be the same or greater than tungsten-based PFCs. To investigate this, a Sn-filled CPS target was exposed to a set of He plasma discharges in Pilot-PSI [11] in the range $q = 1.8$–$18\ MWm^{-2}$ and its performance was examined. Following the set of discharges, it was observed that there was no damage to the underlying W mesh and that the sample remained wetted by the Sn [50]. No macroscopic erosion, i.e. droplet production, was produced due to the small pore size which provided sufficient capillary restraint. Extrapolation of the performance of such a Sn-filled CPS system by modifying mono block designs towards DEMO using COMSOL finite element modelling was done [51] indicating the potential of this PFC solution. Indeed heat loads in the range 15–20 MWm^{-2} could be sustained, dependent on the design, without exceeding the temperature limits for Sn evaporation and those of other materials in the component (figure 5). Further studies are required to qualify the concept for the DEMO divertor.

7. Summary

WP PFC is addressing the most urgent questions in the area of plasma–wall interaction in depth and it complements studies at the major European tokamaks with metallic PFCs. Progress in physics understanding and verified modelling ensures rising confidence in the operation with Be/W in ITER and W-based PFCs in DEMO. Further studies are focused on the plasma–wall interaction in the complex regime with multiple impurities, with neutron damage, and with advanced plasma-facing materials.

Acknowledgments

This work has been carried out within the framework of the EUROfusion Consortium and has received funding from the Euratom research and training programme 2014-2018 under grant agreement No 633053. The views and opinions expressed herein do not necessarily reflect those of the European Commission.

ORCID iDs

S. Brezinsek https://orcid.org/0000-0002-7213-3326
J.W. Coenen https://orcid.org/0000-0002-8579-908X
M. Reinhart https://orcid.org/0000-0002-6436-2129
E. Alves https://orcid.org/0000-0003-0633-8937
T. Angot https://orcid.org/0000-0001-9152-6240
R. Arredondo Parra https://orcid.org/0000-0002-6802-8523
F. Aumayr https://orcid.org/0000-0002-9788-0934
R. Bisson https://orcid.org/0000-0002-8819-1563
D. Borodin https://orcid.org/0000-0001-8354-1387
J. Butikova https://orcid.org/0000-0002-8203-2502
B. Butoi https://orcid.org/0000-0002-2780-1751
N. Catarino https://orcid.org/0000-0003-3879-1533
L. Ciupinski https://orcid.org/0000-0002-4536-3177
M. De Angeli https://orcid.org/0000-0002-7779-7842
D. Dellasega https://orcid.org/0000-0002-7389-9307
P. Dinca https://orcid.org/0000-0003-4383-9941
P. Hansen https://orcid.org/0000-0003-0099-6293
L. Gao https://orcid.org/0000-0003-2514-8514
P. Gasior https://orcid.org/0000-0002-4878-7653
T. Höschen https://orcid.org/0000-0002-4966-1091
W. Jacob https://orcid.org/0000-0003-3504-142X
A. Kaiser https://orcid.org/0000-0002-9439-9176
M. Kelemen https://orcid.org/0000-0002-9972-7909
A. Kreter https://orcid.org/0000-0003-3886-1415
A. Lasa https://orcid.org/0000-0002-6435-1884
N. Lemahieu https://orcid.org/0000-0002-4197-9214
A. Litnovsky https://orcid.org/0000-0001-9791-4316
Ch. Linsmeier https://orcid.org/0000-0003-0404-7191
T. Loewenhoff https://orcid.org/0000-0001-7273-4327
C. Lungu https://orcid.org/0000-0003-2955-0009
L. Marot https://orcid.org/0000-0002-1529-9362
R. Mateus https://orcid.org/0000-0001-6733-6359
D. Matveev https://orcid.org/0000-0001-6129-8427
M. Mayer https://orcid.org/0000-0002-5337-6963
S. Möller https://orcid.org/0000-0002-7948-4305
T.W. Morgan https://orcid.org/0000-0002-5066-015X
J. Mougenot https://orcid.org/0000-0001-7397-0102
R. Neu https://orcid.org/0000-0002-6062-1955
K. Nordlund https://orcid.org/0000-0001-6244-1942
P. Paris https://orcid.org/0000-0002-0829-7510
M. Passoni https://orcid.org/0000-0002-7844-3691
P. Pelicon https://orcid.org/0000-0003-2469-3342
G. Pintsuk https://orcid.org/0000-0001-5552-5427
G. Popa https://orcid.org/0000-0001-9517-385X
C. Porosnicu https://orcid.org/0000-0003-0561-0644
M. Rasinski https://orcid.org/0000-0001-6277-4421
D. Reiser https://orcid.org/0000-0002-2667-4818
G. Riva https://orcid.org/0000-0001-9687-1633
G. Sergienko https://orcid.org/0000-0002-1539-4909
B. Spilker https://orcid.org/0000-0001-9921-0291
P. Ström https://orcid.org/0000-0001-9299-3262
V. Tiron https://orcid.org/0000-0002-2803-1277
P. Tolias https://orcid.org/0000-0001-9632-8104
D. Tskhakaya https://orcid.org/0000-0002-4229-0961
B. Unterberg https://orcid.org/0000-0003-0866-957X
P. Vavpetič https://orcid.org/0000-0001-6204-7435
I.L. Velicu https://orcid.org/0000-0002-7236-2495
A. Weckmann https://orcid.org/0000-0003-1062-8101
M. Wirtz https://orcid.org/0000-0002-1857-688X
R. Zaplotnik https://orcid.org/0000-0002-1366-9147

References

[1] Romanelli F. *et al* 2012 A roadmap to the realisation of fusion energy (EFDA)
[2] Wiesen S. *et al* 2016 *Nucl. Mater. Energy* (https://doi.org/10.1016/j.nme.2017.03.033)
[3] Nordlund K. *et al* 2014 *J. Phys. D: Appl. Phys.* **47** 224018
[4] Kirschner A. *et al* 2015 *J. Nucl. Mater.* **463** S116
[5] Schmid K. *et al* 2015 *J. Nucl. Mater.* **463** S66
[6] Ciarolo G. *et al* 2016 submitted to *Nucl. Mater. Energy* (presented at PSI conference Rom)
[7] Wischmeier M. *et al* 2015 *J. Nucl. Mater.* **463** 22
[8] Majerus P. *et al* 2005 *Fusion Eng. Des.* **75–9** 365–9
[9] Greuner H. *et al* 2007 *J. Nucl. Mater.* **367–70** 1444
[10] Kreter A. *et al* 2015 *Fusion Sci. Technol.* **68** 8
[11] van Rooij G.J. *et al* 2007 *Appl. Phys. Lett.* **90** 121501
[12] Brezinsek S. *et al* 2015 *J. Nucl. Mater.* **463** 11
[13] Kallenbach A. *et al* 2013 *Plasma Phys. Control. Fusion* **55** 12404
[14] Bucalossi J. *et al* 2014 *Fusion Eng. Des.* **89** 907
[15] Philipps V. *et al* 2003 *Plasma Phys. Control. Fusion* **45** S12A A17
[16] Pitts R.A. *et al* 2016 *Nucl. Mater. Energy* (https://doi.org/10.1016/j.nme.2017.03.005)
[17] Rieth M. *et al* 2013 *J. Nucl. Mater.* **432** 482
[18] Piip K. *et al* 2015 *J. Nucl. Mater.* **463** 919
[19] Reimerdes H. *et al* 2015 *42nd EPS Plasma Physics (Lisbon, Portugal, ECA)* vol 39E P4.117 (http://ocs.ciemat.es/EPS2015PAP/html/contrib.html)
[20] Wirtz M. *et al* 2016 *Nucl. Mater. Energy* (https://doi.org/10.1016/j.nme.2016.12.024)
[21] Wirtz M. *et al* 2015 *Nucl. Fusion* **55** 123017
[22] Tolias P. *et al* 2016 *Plasma Phys. Control. Fusion* **58** 025009
[23] Brezinsek S. *et al* 2013 *Nucl. Fusion* **53** 083023
[24] Kirschner A. *et al* 2017 *Plasma Phys. Control. Fusion* submitted
[25] Tskhakaya D. *et al* 2013 *J. Nucl. Mater.* **438** S522
[26] Moulton D. *et al* 2013 *Plasma Phys. Control. Fusion* **55** 085003
[27] Dobes K. *et al* 2014 *Nucl. Instrum. Methods. Phys. Res.* B **340** 34
[28] Gao L. *et al* 2015 *Nucl. Fusion* **56** 016004
[29] Drenik A. *et al* 2016 *J. Nucl. Mater.* **475** 237
[30] Laguardia L. *et al* 2016 *Nucl. Mater. Energy* (https://doi.org/10.1016/j.nme.2017.05.009)
[31] Dittmar T. *et al* 2016 private communication
[32] de Castro A. *et al* 2015 *J. Nucl. Mater.* **463** 676
[33] Jepu J. *et al* 2015 *J. Nucl. Mater.* **463** 983
[34] Dinca P. *et al* 2017 *Surf. Coat. Technol.* **321** 397–402
[35] Mateus R. *et al* 2016 *Fusion Energy Des.* (https://doi.org/10.1016/j.fusengdes.2017.01.018)
[36] Pribula M. *et al* 2016 *Phys. Scr.* **T167** 01404
[37] Colao F. *et al* 2016 *Nucl. Mater. Energy* (https://doi.org/10.1016/j.nme.2017.05.010)
[38] Xi J. *et al* 2016 *Nucl. Mater. Energy* (https://doi.org/10.1016/j.nme.2016.11.021)
[39] Zlobinski M. *et al* 2011 *Phys. Scripta* **T145** 014027
[40] Hodille E.A. *et al* 2017 *Nucl. Fusion* **57** 076019
[41] Schmid K. *et al* 2016 *Phys. Scr.* **T167** 014025

[42] Kato D. *et al* 2015 *Nucl. Fusion* **55** 083019
[43] Markelj S. *et al* 2016 *Nucl. Mater. Energy* (https://doi.org/10.1016/j.nme.2016.11.010)
[44] Sugiyama K. *et al* 2015 *J. Nucl. Mater.* **463** 272
[45] Ström P. *et al* 2016 *Nucl. Instrum Methods Phys. Res.* B **371** 355
[46] Roth J. *et al* 2014 *J. Nucl. Mater.* **454** 1
[47] von Toussaint U. *et al* 2016 *Phys. Scr.* **T167** 014023
[48] Tabares F.L. *et al* 2016 *Nucl. Mater. Energy* (https://doi.org/10.1016/j.nme.2016.11.026)
[49] Oyarzabal E. *et al* 2015 *J. Nucl. Mater.* **463** 1173
[50] Morgan T. *et al* 2016 *Nucl. Mater. Energy* (https://doi.org/10.1016/j.nme.2017.01.017)
[51] Li-Puma A. *et al* 2013 *Fusion Eng. Des.* **88** 1836–43